# Original Paper

## Modelling of sand grain dissolution in industrial glass melting tanks

Ruud G. C. Beerkens, Hendricus P. H. Muijsenberg and Tom van der Heijden

TNO Institute of Applied Physics, Eindhoven (The Netherlands)

A combination of two models, describing dissolution of sand grains in batch blankets or in the molten glass, is presented: a microscale and a macroscale model. The macroscale model is based on a 3-dimensional calculation procedure to determine the temperature distributions and the flows in industrial glass melting tanks. By means of microscale models, using mass transfer relations for diffusional transport, the dissolution rate of single sand grains can be calculated. The dissolution of the sand is determined by following a large number of single grains during their trajectories through the batch blanket and the molten glass in the glass melting tanks.

The dissolution rate of a sand grain is calculated for the temperatures and flow conditions in every volume element in the tank through which the grain proceeds. The dissolution rate in the batch blanket depends strongly on temperature and the stage of the dissolution process. Initially the very fast shrinkage rate of the grains as temperatures exceed 1200 °C results within 10 min in the dissolution of more than 50 % of the sand in the blanket.

Forced and free convection in the glass melt leads to increases in the dissolution rate, up to a factor 5 compared to motion-free conditions. Forced bubbling for instance results locally in extremely high mass transfer rates and often improves the melting performance of industrial glass furnaces.

**Modell der Auflösung von Sandkörnern in industriellen Glasschmelzöfen**

Zur Ermittlung der Auflösungsgeschwindigkeit von Sandkörnern im Gemengeteppich und in der Glasschmelze wurden zwei mathematische Modelle kombiniert: ein Modell zur Beschreibung des Verhaltens von einzelnen Körnern in ihrer Umgebung und ein Modell zur Berechnung der Temperaturverteilung und der Strömungsbedingungen im Schmelzaggregat. Das erste Modell basiert auf Massentransportgleichungen, mit deren Hilfe die Diffusion von $SiO_2$ in der Schmelze und damit die Auflösungsgeschwindigkeit einzelner Sandkörner bestimmt werden können. Die Auflösung des Sandes wird ermittelt, indem man den Weg einer größeren Anzahl von Einzelkörnern zunächst durch den Gemengeteppich und dann durch die Schmelze verfolgt. Die Auflösungsgeschwindigkeit eines Sandkorns wird in denjenigen Volumenelementen des Glasschmelzofens berechnet, durch den das Korn wandert, und zwar unter Berücksichtigung der in den jeweiligen Volumenelementen herrschenden Temperaturen und Strömungsbedingungen. Die anfangs sehr hohe Auflösungsgeschwindigkeit bei Temperaturen oberhalb von 1200 °C bewirkt, daß sich innerhalb von 10 min mehr als 50 % des Sandes in der Gemengedecke lösen. Die erzwungene und freie Dichtekonvektion in der Glasschmelze führt zu einer Beschleunigung der Auflösungsgeschwindigkeit um den Faktor 5, verglichen mit konvektionsfreier Auflösung. So ruft z.B. das bewußte Lufteinblasen (Bubbling) lokal sehr hohe Massentransportraten hervor und verbessert damit oft das Einschmelzverhalten in industriellen Glasschmelzöfen.

### 1. Introduction

The manufacturing of glass products without seeds, inhomogeneities and undissolved batch materials is of major concern for the glass technologist. The effects of changes in glass or batch composition, batch blanket performance, temperature levels and glass melt flows in industrial melting tanks on the dissolution of sand grains is only poorly understood and mainly based on empirical experiences.

In this paper a method is presented to simulate mathematically the behaviour of dissolving sand grains, by means of mass transfer equations [1 to 11] and flow modelling [12 to 18]. With this method, the trajectories in the melting tank through the batch blanket and into the melt and the individual dissolution rates for large quantities of single sand grains can be calculated. The amount of still undissolved material or the sizes of undissolved sand grains in the throat of the furnace or at other locations can be calculated following the procedure given in this paper.

In sections 2.1. and 2.2. two microscale models are presented to calculate the mass transfer of dissolving $SiO_2$ grains in the batch blanket and in the melt.

In order to apply these single grain models to industrial situations, the glass flows, the temperature distribution, and the trajectories of the grains in the tank have to be known. Section 3. describes the 3-D macromodelling of the glass flows and temperature distribution in melting tanks. The single grain model can then be applied as a post-process model, calculating the dissolution of a grain during its trajectory in the tank. The dissolution rates of a large amount of single sand grains in industrial furnaces following the calculated flow patterns for these grains and temperature fields are determined by the mass transfer relations given in the micromodels.

Received October 21, 1993.

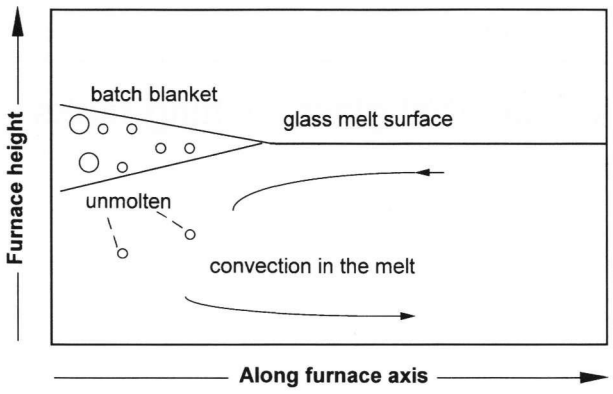


Figure 1. Position of batch blanket floating on the glass melt in an industrial glass furnace.

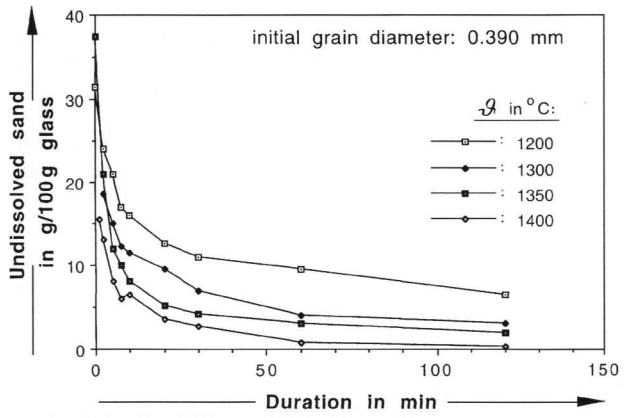


Figure 2. Dissolution of sand grains in isothermally heated batches.

By this simulation method, the influence of the furnace design and the effects of different process conditions in the furnace on the performance of the melting tank and the melting quality can be derived.

The diffusion of dissolved silica in the liquid molten glass often determines the shrinkage rate of sand grains in the glass melt. Only in the early stages of dissolution in the batch blanket, the rate may be limited by reaction kinetics. At the sand grain surface, reactions take place between solid $SiO_2$ and the alkali- or earth alkali-rich silicate phases surrounding these grains. Sand grains located in the batch blanket of industrial furnaces partly dissolve before entering the glass melt adjacent to the blanket. This process may be partly controlled by the heat transfer in the batch blanket [19 and 20], by reaction kinetics and also by diffusion of dissolved $SiO_2$ into the liquid phases.

The remaining sand grains entrained in the glass melt on which the batch blanket floats dissolve mainly by a diffusion-controlled process, which can be enhanced by convection of the melt. Figure 1 schematically shows the situation of the batch blanket and the melt in an industrial continuous melting process.

## 2. Isothermal studies on sand grain dissolution in glass batches

An experimental study of the dissolution of sand grains during isothermal treatment of small quantities of raw material batches has been performed analogously to the investigations done by Bènes [1] and described by Hrma et al. [2].

In the laboratory study raw material batches mixed to prepare an industrial glass of the composition (in wt%): 57 $SiO_2$, 13.7 $Al_2O_3$, 22 CaO, 5 $B_2O_3$ and small amounts of $SO_3$, $Fe_2O_3$, $K_2O$ and $Na_2O$ have been melted in charges of 20 g. Sand fractions of a narrow grain size distribution have been used.

Platinum crucibles containing these batches were placed in electrical furnaces, preheated up to the desired melting temperature. After a duration of 2.5, 5, 7.5, 10, 20, 30, 60 or 120 min, the crucible was rapidly cooled down to room temperature. The obtained glass/sand mixture has been ground and brought into a $H_2SiF_6$ solution. The glassy phases dissolve in these solutions, whereas the residue of sand grains remains intact. After filtration the amount of undissolved sand residue has been measured gravimetrically.

In figure 2 the dissolution kinetics of sand grains, with initial diameters of 390 µm has been given for a few melting temperatures as a function of time. During the first stage (0 to 10 min) dissolution proceeds very fast, this period is comparable with the situation in the batch blanket, where an aggressive primary melting phase has been formed. The decrease of the fraction of undissolved sand in the sand/melt mixture is approximately proportional to the time in this early stage. The last 20 to 50 % of the sand dissolves relatively slowly, especially at temperatures below 1300 °C.

### 2.1. Dissolution in the batch blanket

In the models of the sand grain dissolution process, it has been assumed that the grains have a spherical shape and a smooth surface.

Preliminary experiments with the raw material batches have shown that the dissolution of sand grains is the most critical process in obtaining a product without undissolved material. Above 1100 °C all raw materials other than sand in these batches were absorbed in the liquid phases within 5 to 10 min. In the models it has been assumed that all raw material constituents other than sand dissolve instantaneously. However, sometimes this may be not true especially for alumina-rich and coarse raw materials. The dissolution process consists of two stages:

a) The reaction at the grain surface of the crystalline or amorphous silica with the alkali- or earth alkali-rich liquid silicate phase.

b) The diffusion of the silica-rich reaction product from the surface into the liquid phase, considered as $SiO_2$ diffusion. The diffusion is characterized by a pseudo-binary interdiffusivity of $SiO_2$ in a melt consisting of the other glass constituents.

These two processes may be considered as a serial sequence of mass transfer processes. Hrma et al. [2], Mühlbauer et al. [3] and also Beerkens [4] applied this approach to explain experimental observations.

### 2.1.1. Cases without convection

The total resistance to the mass transfer of $SiO_2$ from the sand grain into the bulk of the melt is the sum of the resistance due to the limited reaction kinetics and the resistance by the diffusion process,

$$1/h_{rd1} \equiv 1/h_r + 1/h_d \,. \tag{1}$$

The shrinkage rate of the sand grain during dissolution in the batch blanket is given by:

$$\varrho_s \cdot \frac{dR}{dt} \equiv -h_{rd1} \cdot (\varrho_e \cdot w_e - \varrho_b \cdot w_b) \,. \tag{2}$$

Here, equation (2) is approximated using a corrected $h_{rd}$ value by:

$$\frac{dR}{dt} = -h_{rd} \cdot (w_e - w_b) \,. \tag{3}$$

The value of $h_r$ for a given batch composition is considered to be only dependent on the temperature and has to be determined by experiments. The rate of diffusion depends on the $SiO_2$ diffusivity in the melt, represented by a mean value $D_m$, and the $SiO_2$ concentration gradient, which depends on the duration of the diffusion process and on the convection of the melt. Doremus [5] showed that for a process, controlled by diffusion only, without convection, the initially very fast shrinkage rate diminishes because of the flattening of the concentration profile or the increase in diffusion boundary layer thickness in the melt surrounding the grain.

For the quasi-stationary isothermal situation, Weinberg et al. [6] gave the following relation for the mass transfer coefficient determined by the time-dependent diffusion:

$$h_d = D_m \cdot (1/R + 1/\sqrt{(\pi \cdot D_m \cdot t)}) \,. \tag{4}$$

### 2.1.2. Cases with convection

Two other phenomena have to be considered in this formulation of the dissolution process:

a) The influence of the moving boundary of the grain/melt interface by the shrinkage process. According to Ready and Cooper [7] and Cooper and Kingery [8], this leads to a convection of the melt in radial direction, which often enhances the dissolution rate by roughly a factor $1/(1 - V_s \cdot c_e)$. $V_s$ is the specific partial volume of $SiO_2$ in the melt and $c_e$ is the equilibrium concentration of $SiO_2$ in the melt at the interface of the sand grain.

b) The density in the liquid phase near the dissolving grains generally differs from the density in the bulk of the melt. Choudhary [9 and 10] has shown that free convection driven by these density gradients considerably effects the dissolution behaviour. To account for the free convection, $h_d$ is approximated by substituting in equation (4), for $D_m$ the term $D_m \cdot Sh/2$ ($Sh$ = the Sherwood number) and for $\pi \cdot D_m \cdot t$:

the term $R_h = \pi \cdot \int_0^t D_m \cdot Sh/2 \, dt$ .

$R_h$ is a history term, which accounts for the shape of the $SiO_2$ concentration profile in the melt. This profile depends on time ($t$), on convection ($Sh$), and on the diffusivity ($D_m$). The profile is relatively steep for low diffusivities, short times, and no convection. Including convection, equation (4) has to be replaced by:

$$h_d \equiv D_m \cdot Sh/2 \cdot (1/R + 1/R_h) \,. \tag{5}$$

The Sherwood number for free convection, neglecting forced convection in the batch blanket, can be derived by Choudhary's method [9 and 10] and general mass transfer relations [11], neglecting other convective contributions:

$$Sh_g = 2 + 0.89 \cdot Gr^{1/3} \cdot Sc^{1/4} \,. \tag{6}$$

The Grashof and Schmidt numbers can be calculated by:

$$Gr \equiv 8 \cdot g \cdot R^3 \cdot \varrho_b \cdot (\varrho_b - \varrho_e)/\mu_b^2 \,, \tag{7}$$

$$Sc \equiv \mu_b/(D_m \cdot \varrho_b) \,. \tag{8}$$

The effect of the 'moving grain boundary' on the mass transfer of $SiO_2$ into the melt may be incorporated by multiplying $h_d$ by a factor $1/(1 - V_s \cdot c_e)$. This term takes into account the radial convection in the melt due to a change of the occupied volume of $SiO_2$ in the melt compared to the specific volume of $SiO_2$ in the grains.

Finally the overall mass transfer coefficient is given by:

$$h_{ov} = 1/[(1/h_d + 1/h_r) \cdot (1 - V_s \cdot c_e)] \,. \tag{9}$$

The maximum mass fraction of $SiO_2$ which can be dissolved in the melt is determined by thermodynamics and called the $SiO_2$ solubility $w_e$. The value of $w_e$ depends for a given glass composition only on the temperature. Generally $w_e$ increases with temperature.

For the glass composition mentioned earlier, the experimentally derived temperature dependency is presented by:

$$w_e \equiv 0.000475 \cdot T - 0.1227 \tag{10}$$

with $T$ in K.

The parameter $w_b$ is the mass fraction of dissolved $SiO_2$ in the melt. Defining $w_t$ as the mass fraction of undissolved sand in the glass/sand mixture, $w_0$ the mass fraction of undissolved sand in this mixture at $t = 0$, and $w_{ns}$ the mass fraction of $SiO_2$ dissolved in the melt but originating from other constituents than sand

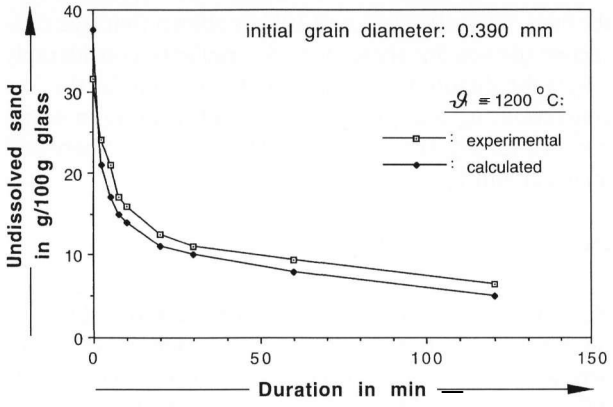


Figure 3. Dissolution of sand grains ($D_0$ = 390 µm) in a glass batch at 1200 °C according to experimental results and model calculations.

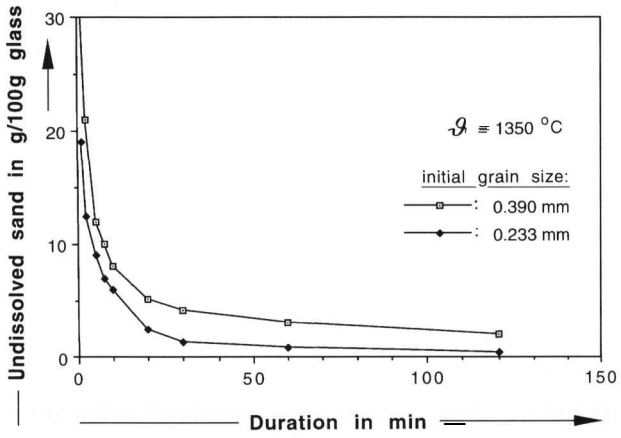


Figure 4. Dissolution of monodisperse sand in isothermally heated glass batches for two initial grain sizes.

$$w_b = (w_0 - w_t)/(1 - w_t) + w_{ns}/(1 - w_t) \quad (11)$$

with

$$w_t = w_0 \cdot (R/R_0)^3 \quad \text{(for monodisperse sand)} . \quad (12)$$

$R_0$ is the initial radius of the monodisperse sand in the batch. The radius $R$ of the sand grains decreases with time, which leads to an increase in the value of $w_b$. Thus, the 'driving force' for the dissolution process ($w_e - w_b$) decreases with time for an isothermal process.

### 2.1.3. General formulation for sand grain dissolution during heating of the batch

Combining equations (3, 11 and 12) and replacing $h_0$ for $h_t$, a general expression for the dissolution of monodisperse sand grains in batch blankets is obtained:

$$\frac{dR}{dt} = -h_{ov} \cdot [w_e - \{w_{ns} + w_0 \cdot (1 - R^3/R_0^3)\}/(1 - w_0 \cdot R^3/R_0^3)] . \quad (13)$$

Equation (13) can easily be modified for bidisperse or multidisperse sands.

The values $w_0$, $w_{ns}$ and $R_0$ are known from the batch composition, $w_e$ has to be derived experimentally. In figure 3 results of calculations for isothermally heated batches are compared with results of experiments discussed at the beginning of section 2.

From figure 3 the following conclusions can be drawn:

- The calculation procedure is an adequate and predictable way to determine the dissolution kinetics of sand grains in isothermally heated batches.
- More than 50 % of the sand dissolve in the first stage lasting about 10 min. This period represents the batch blanket situation.
- $dw_t/dt$, the slope of the fraction of undissolved sand with respect to time, is nearly linear in the early stages. It appears that the slope depends only on the initial grain size and the temperature.

Instead of using this complicated calculation procedure for the case of sand dissolution in the batch blanket, an empirical equation can be used as an approximation:

$$dw_t/dt = C_1 \cdot \exp(B - T)/C \quad \text{for} \quad T > B \quad (14)$$

or

$$dR/dt = 1/3 \cdot R_0^3/R^2 \cdot A \cdot \exp(B - T)/C . \quad (15)$$

Relation (15) has to be applied to $T > B$, else $dR/dt = 0$. Below the temperature $B$ no sand grain dissolution takes place.

The values of $C_1$, $B$ and $C$ have been derived for this glass batch from figure 2, the value of $A$ has been derived using equation (12). For this case: $A = 0.000002\ s^{-1}$, $B = 1100$ K, $C = 50$ K.

The influence of the initial grain size on the dissolution rate of sand grains is shown by figure 4.

## 2.2. Dissolution process in the molten glass

Single sand grains may penetrate from the batch blanket into the glass melt adjacent to this blanket. The dissolution of the grains continues, but is now hardly limited by the reaction kinetics of the conversion of silica into silicates. The dissolution rate is mainly controlled by the interdiffusion of $SiO_2$ into the melt. This process is often enhanced by the convection in industrial melting tanks.

Again, the dissolution rate can be described by an equation such as relation (2):

$$\varrho_s \cdot \frac{dR}{dt} = -h_m \cdot (\varrho_e \cdot w_e - \varrho_b \cdot w_b) . \quad (16)$$

In equation (16) the mass transfer coefficient $h_m$ depends on free and forced convection and the pseudobinary diffusivity of $SiO_2$ in the melt. The value of $w_b$ is approximately constant because the molten glass which has been separated from the batch blanket nearly reaches its final composition.

The mass transfer coefficient $h_m$ in the melt depends on:

a) the mean effective (pseudobinary) interdiffusivity of dissolved $SiO_2$ in the melt, which has been derived experimentally;

b) free convection, introduced by density differences in the liquid phase between locations with high $SiO_2$ concentrations ($w_e$) and lower $SiO_2$ concentrations ($w_b$);

c) forced convection, as a result of the flow patterns in the melting tanks. The flow currents in the melt are a result of forced bubbling or temperature differences in the tank;

d) the stage of the dissolution process: Initially the concentration profile of $SiO_2$ dissolved in the melt surrounding a grain is very steep, but flattens at increasing time. This flattening of the concentration profile results in a quasi-steady state profile. Especially in cases where free and forced convection are involved, the dissolution can be approached by the quasi-steady state formulation;

e) the radial convection of the melt surrounding a sand grain due to the moving grain/melt interface and the dissolution process itself; therefore, the dissolution rate is enhanced by a factor $1/(1 - V_s \cdot c_e)$.

### 2.2.1. Quasi-steady state approach

The dissolution rate in the quasi-steady state without convection is calculated by:

$$\frac{dR}{dt} = -D_m/R \cdot 1/\varrho_s \cdot (\varrho_e \cdot w_e - \varrho_b \cdot w_b) . \quad (17)$$

The enhancement of the dissolution process through convective contributions can be attributed for, by multiplication of the right term in equation (17) by $Sh/2$.

A sand grain moves with the velocity which prevails at the position of the centre of the grain plus the rising velocity caused by the density difference between the silica grain and the silicate melt. The Sherwood number depends on the density differences in the melt surrounding the dissolving grain (free convection) and the velocity profile in the melt (forced convection).

### 2.2.2. Effects of free convection on the dissolution process

The Sherwood number ($Sh_g$) for free convection plus convection introduced by the moving grain boundary is approximated by relations for spherical symmetry [10 and 11]:

$$Sh_g = (2 + 0.89 \cdot Gr^{1/3} \cdot Sc^{1/4})/(1 - V_s \cdot c_e) ; \quad (18)$$

$$Gr = 8 \cdot g \cdot \varrho_b \cdot (\varrho_b - \varrho_e) \cdot R^3/\mu_b^2 ; \quad (19)$$

$$Sc = \mu_b/(\varrho_b \cdot D_m) . \quad (20)$$

In equations (18 to 20), the index b refers to the bulk of the melt and the index e to the melt bounded by the grain surface.

### 2.2.3. Effects of forced convection on the dissolution process

Flow currents in the melting tank lead to velocity gradients. The sand grains with a lower density than the molten glass ascend relatively to the surrounding melt. The velocity gradients in the melt and the ascension of the grains lead to a reduction in the boundary layer thickness surrounding the grain and thus a steeper $SiO_2$ concentration profile. During this process cords of silica-rich phases may be formed. The dissolution of the sand grains is enhanced by the convection which stretches the $SiO_2$-rich layer.

A sand grain moves with the velocity which prevails at the position of the centre of the grain plus the rising velocity caused by the density difference between the silica grain and the silicate melt. The value for the velocity of a sand grain relative to the melt is approximately determined by the following procedure:

From the 3-dimensional macromodel the velocity gradients of the melt in the $x$, $y$, and $z$ direction are known at any arbitrary position in the melting tank. The absolute velocity of a sand grain relative to the surrounding melt, neglecting the ascension of the grain relative to the melt, can be calculated by:

$$v_a = [(R \cdot dv_x/dx)^2 + (R \cdot dv_y/dy)^2 + (R \cdot dv_z/dz)^2]^{1/2} . \quad (21)$$

Using the results of the macroscale 3-D modelling of the melting tank, $v_a$ can be derived for every grain at every position in the furnace.

The extra rising velocity $v_s$, due to the lower density of the grain, may be calculated by the expression valid for Stokes' flow conditions:

$$v_s = 2/9 \cdot (\varrho_b - \varrho_s) \cdot g \cdot R^2/\mu_b . \quad (22)$$

The absolute value for the velocity of the grain relative to the melt, $v_t$ is obtained by the combination of $v_a$ and $v_s$. Now the Reynolds number is approximated by:

$$Re = v_t \cdot d_p \cdot \varrho_b/\mu_b . \quad (23)$$

In this equation $d_p$, the grain diameter is equal to 2 $R$.

The Sherwood number for forced convection ($Sh_{mb}$) around spherical objects, taking the radial convection caused by the moving grain boundary into account, is given by:

$$Sh_{mb} = (2 + 0.89 \cdot (Re \cdot Sc)^{1/3})/(1 - V_s \cdot c_e) . \quad (24)$$

### 2.2.4. Combination of free and forced convection contributions

In practice, both free and forced convection have an impact on the mass transfer processes in the melting tank. The Sherwood number which incorporates both effects can be estimated by:

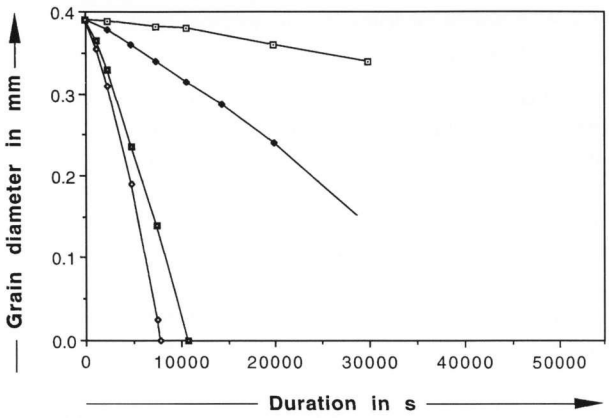


Figure 5. Reduction of sand grain diameter during the dissolution process in the glass melt. □: without convection, ◆: only free convection, ■: forced convection with a velocity gradient of $0.5\,s^{-1}$, ◇: forced convection with a velocity gradient of $1\,s^{-1}$.

Table 1. Important furnace and process data used for model calculations

| | |
|---|---|
| glass | soda–lime–silica glass |
| pull rate | 200 t/d |
| cullet | 40% |
| furnace | container glass unit melter |
| length of melter | ±20 m |
| width of melter | ±6.0 m |
| height of molten glass | ±1.10 m |
| position of bubblers | in bottom at 10 m from batch input distributed over the width of the tank |
| mean residence time | 28 h |
| maximum crown temperature | 1565 °C hot spot |
| components of batch | sand<br>soda<br>lime<br>sodium sulphate<br>feldspars |

$$Sh = (2 + 0.89 \cdot [Re \cdot Sc + (Gr \cdot Sc^{3/4})]^{1/3})/(1 - V_s \cdot c_e) \,. \quad (25)$$

Finally, the dissolution rate of single sand grains in the molten glass can be derived at any position by:

$$\frac{dR}{dt} = -D_m/(2 \cdot R) \cdot Sh/\varrho_s \cdot (\varrho_e \cdot w_e - \varrho_b \cdot w_b) \,. \quad (26)$$

The dissolution behaviour of a single and grain in a molten glass according to the calculations, using the described procedure, has been presented by figure 5. In this example, the temperature of the melt is 1400 °C and the grains have an initial diameter of 390 µm. In figure 5 different cases are given:

a) no convection at all;
b) only free convection;
c) forced convection with a velocity gradient of $0.5\,s^{-1}$;
d) forced convection with a velocity gradient of $1\,s^{-1}$.

## 3. Glass tank modelling and sand grain dissolution

A general 3-dimensional glass tank model has been developed based on finite difference calculation methods at TNO, Eindhoven (The Netherlands). This model is the basis for the complex description of all relevant processes taking place during industrial glass melting. Glass tank modelling has been a topic of intensive study by different researchers in the last decade [12 to 17]. The TNO glass tank flow model describes the heat transfer in the molten glass and the convection patterns. In this model the interaction of the molten glass with the batch blanket, the combustion chamber, furnace walls or obstacles/flow barriers in the tank, electric boosting and the action of forced bubbling are or can be included.

Here some illustrative results for temperature distributions and velocities using this mathematical modelling will be given for a simple industrial furnace design.

The model is applicable for all industrial glass furnace designs.

### 3.1. Flow and heat transfer modelling

This mathematical model [15 to 17] has been developed for the calculation of the molten glass flows and temperatures depending on the position in melting tanks:

- with a given construction and for given furnace dimensions;
- with or without forced bubbling;
- with a batch blanket;
- including local heat sources like electrical boosting;
- with flow barriers or walls;
- having local cooling, like glass line cooling;
- involving the heat transfer from the combustion chamber to the melt surface.

The numerical method has been based on Patankar's finite difference approach [18]. Equations for continuity, energy conservation, and the Navier-Stokes equations are solved numerically. Realistic boundary conditions or interactions of the molten glass with other phases have been implemented in detail. The interaction of the blanket and the molten glass has been described using "apparent viscosities" for the batch floating on the melt. Here examples will be presented for a furnace (table 1) with or without forced bubbling and a flow barrier.

Figure 6 presents an overview of one half of a glass melting tank with a throat, a batch blanket and the glass tank boundaries. The bold line represents the inner dimensions of the tank, the position of the batch blanket has also been indicated. Figures 7a to c illustrate the calculated glass temperature levels in one half of this industrial tank for a melter equipped without and with forced bubbling. The heat penetration in the molten glass in the first case is clearly less than for the case of forced bubbling.

The position of the relatively cold batch blanket can be distinguished (at temperatures <1200 °C), molten glass near the bottom of the tank is mixed by the glass

at the surface by the action of the forced bubbling near the hot spot. This will have two important effects: First, the relatively cold melt at bottom position will be heated by the hot melt from the surface, which improves melting and degassing, but also the temperature of the bottom refractories rises. However, this could increase corrosion rate at these positions. Second, the temperature of the surface decreases. This leads to a higher heat input from the combustion chamber to the "colder" melt surface.

The model involves the calculation of the heat conductivity through the refractory materials and the heat transfer to the surroundings of the furnace. The melt cools down in the throat flowing to the working end. At every position not only temperatures but also local velocities in all three directions have been calculated. Figures 8a and b show the velocity vectors in the molten glass as calculated by flow modelling for a melter with and without forced bubbling.

From this figure, zones may be seen with recirculation or mixing especially near the forced bubbling section with very high velocities, which improve the mixing and the dissolution of unmolten materials. At the surface of the molten glass a very intensive flow of molten glass from the bubblers to the batch blanket can be observed. The relatively hot melt moves to positions below the batch blanket. An important part of the batch will be melted by the heat flux from this molten glass at the tip of the blanket. Batch material will flow in forward direction into the furnace and also from the central part to the sidewalls. In this case a flow of batch material from the blanket centre to the sidewalls and then downwards and back to the batch input area takes place. Piston flow areas can be recognized for instance in the throat.

Glass tank flow modelling only has been hardly applicable for the optimization of the quality of the melting process and the glass products. Therefore, submodels have been prepared using information from more detailed studies given in section 2. of this paper on melting kinetics in molten glass and batch blankets. By these submodels, the dissolution of single sand grains in the tank can be described for calculated temperature levels and flow patterns of the melt.

Particle tracing techniques have been applied, in order to follow, in the modelling, small volumes of molten glass during their trajectories in the melting tank. This technique is very powerful to determine the melting history of different volumes of molten glass and to derive the residence time distribution for a particular tank for predescribed process conditions. Along the trajectory of a volume of molten glass, the local temperature and flow conditions at every position are given by the results of the 3-dimensional glass tank flow modelling. Particle tracing is an important tool to follow mathematically the behaviour of single sand grains during their trajectories in the melt.

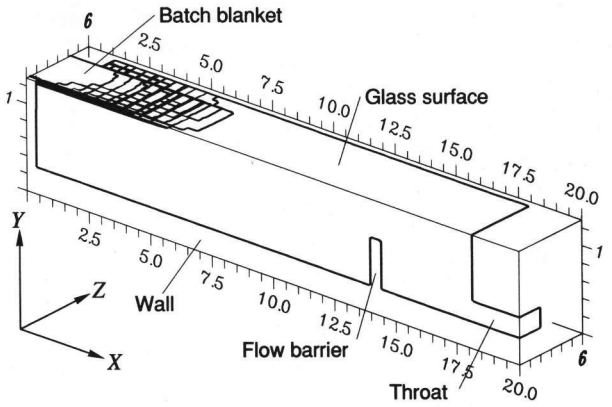


Figure 6. One half of a glass melting tank of a unit melter with batch blanket.

Figure 9 presents illustratively a trajectory of a small volume of material in a glass tank according to modelling, using the particle tracing method for a situation without forced bubbling. The residence time of this volume of glass is 10 h. The volume of material may pass several times some sections in the tank, but it never will cross its own trajectory (which is hardly visible in these 2-dimensional plots). Especially in case of forced bubbling the trajectory of a single small volume of molten glass or a sand grain may be very long but there are also volumes which follow a short cut and these will have very short residence times. In a glass tank without forced bubbling the trajectory and dissolution of the same sand grain is very different compared to the case with forced bubbling showing strong recirculation patterns.

Using this particle tracing method, the melting rate and trajectories of sand grains charged at different positions into the doghouse area can be derived using the sand dissolution submodels in combination with flow modelling.

## 3.2. Sand grain dissolution calculations in tanks

The dissolution rate of sand grains depends very much on the solubility and diffusivity of $SiO_2$ in the molten glass. This solubility and diffusivity is determined by the local temperature and glass composition. However, as demonstrated in section 2., dissolution can be enhanced by forced and free convection [7 to 9]. After the determination of the temperature distribution and flows in the melting tank, the dissolution rate of a single sand grain can be derived at every location in the tank through which the grain is transported by the melt. With this method the dissolution or melting of a large number of different sand grains starting from different positions can be calculated. Figures 10a and b show results of these calculations for a few thousands of grains. In every cross-section the progress of the dissolution of grains is presented using contours indicating the maximum diameter of still undissolved grains.

Figure 10a shows that in the case without forced bubbling there are still undissolved sand particles just before the melt enters the throat. However, in this throat

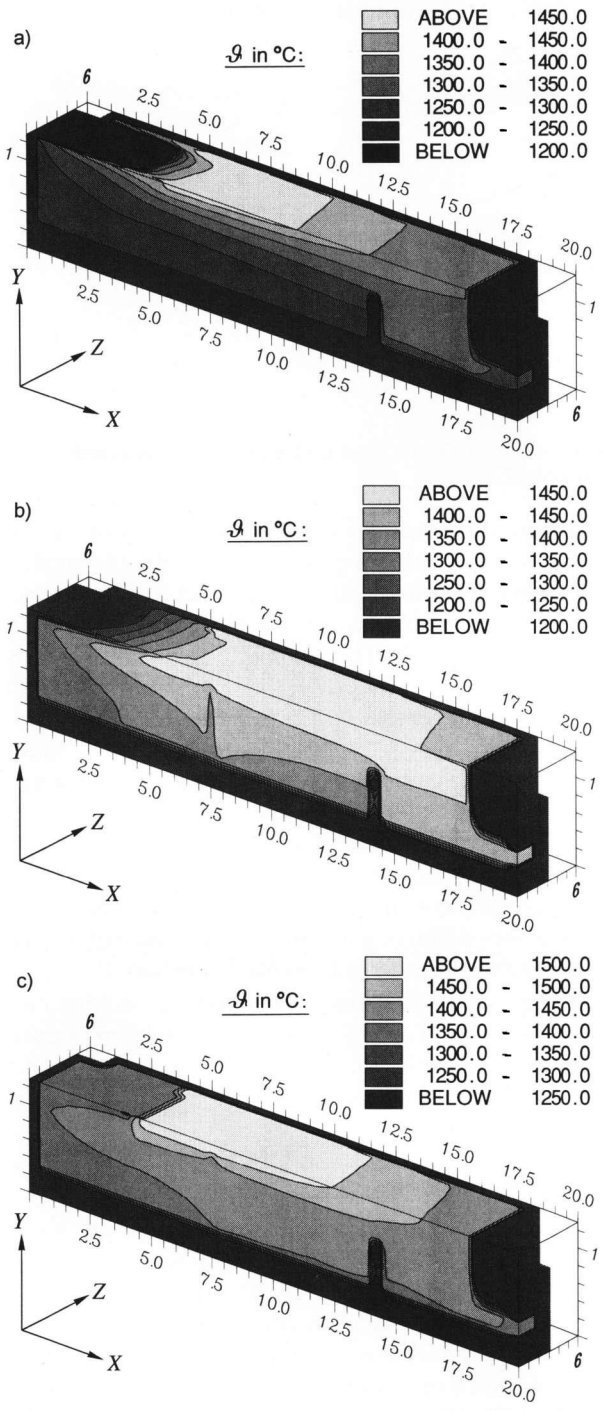


Figures 7a to c. Calculated glass temperature contours for different cases; a) without forced bubbling, b) with forced bubbling, 9 bubblers in line across the width of the tank, c) with forced bubbling and 30 K higher hot spot temperature.

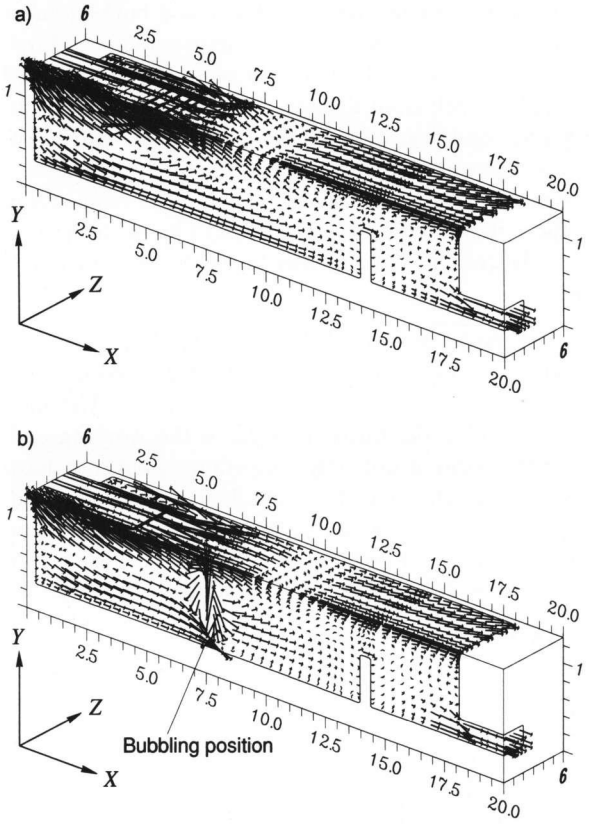


Figures 8a and b. Calculated velocities of molten glass in the tank for two cases; a) without bubbling, b) with forced bubbling.

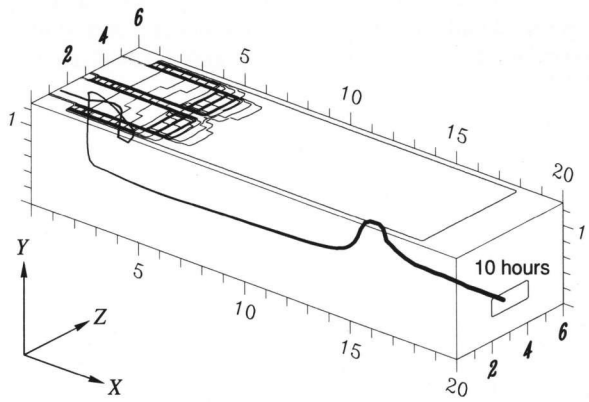


Figure 9. Particle trajectory in a glass melting tank calculated with the tank model for a given initial position in the batch blanket.

the last few grains dissolve completely. In this case the initial diameter of the sand grains regarded here is 0.3 mm, larger sand grains will cause melting problems because then melting at the throat will be incomplete. The dissolution of sand grains depends very much on the temperature and the velocity gradients in the melt. The dissolution rate can be increased by convection by a factor 5 to 10, especially near the bubblers. Figure 10b shows the presence of nondissolved sand grains in the throat for a melter with forced bubbling, using also sand with sand grain diameters of 0.3 mm. As expected, bubbling considerably helps the sand melting/dissolution process.

Figure 11 shows the effect of forced bubbling on the maximum sand grain sizes which can be completely dissolved in this melting tank under the conditions given in table 1. A bubbler row with nine bubblers in line has

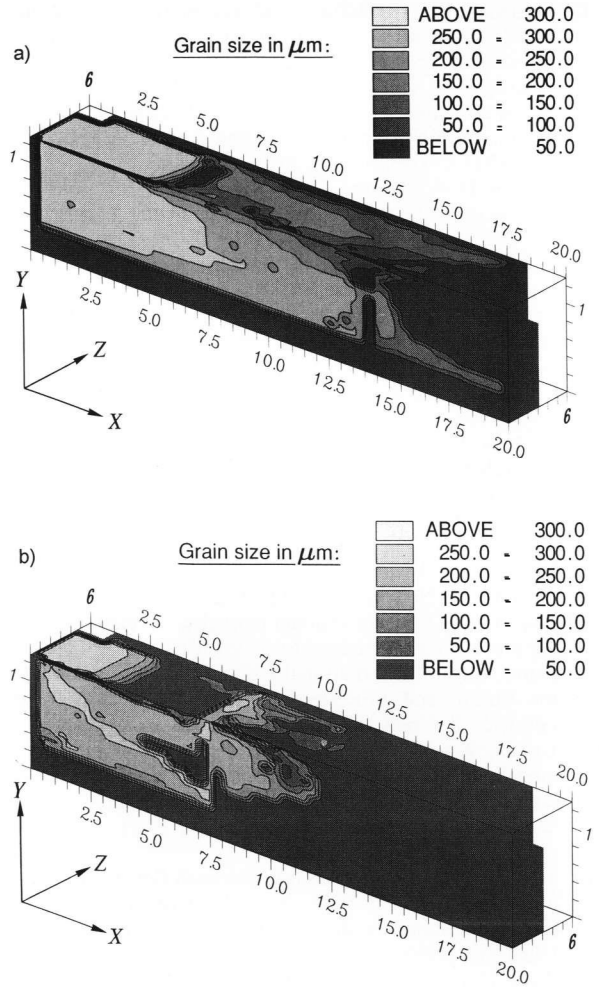


Figures 10a and b. Largest undissolved sand grain in flint soda–lime glass melting tanks indicated by contours for three different cases; a) without bubbling, maximum crown temperature 1565 °C, b) forced bubbling, 0.72 l/min (at 273 K, 1 bar) per bubbler; initial sand grain diameter 300 μm.

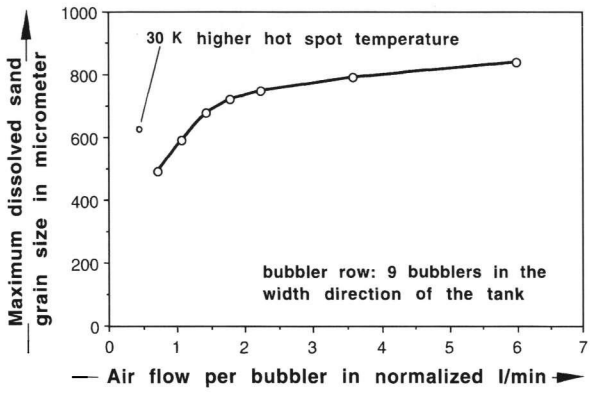


Figure 11. Effect of forced bubbling rate on maximum sand grain size in flint soda–lime glass which can be completely melted in the tank.

been included in the modelling. The melting performance of this tank will already be improved by moderate bubbling.

Above 3 l/min (normalized 273 K, 1 bar) of air per bubbler, a further increment in bubbling rate will have a minor impact on melting kinetics and may be dangerous for the refractories or may affect the fining process. A 30 K higher hot spot temperature of the furnace will have an important effect on the maximum sand grain size which can be completely dissolved.

The here presented method of glass tank modelling, including post-process modelling of sand grain dissolution, appears to be a very important tool to study the influence of grain size, forced bubbling but also electric boosting, pull rate, temperature levels and the location and shape of the batch blanket on the melting quality in industrial furnaces.

## 4. Conclusions

The effect of changes in the furnace geometry, furnace dimensions, intensity of forced bubbling, the position of forced bubbling, the positions of flow barriers, the distribution of the fuel over the different burners, the action of electric boosting or batch composition on the quality of the melting process can be studied using detailed models based on fundamental knowledge of the chemical and physical processes in the glass melting tank. Initial grain size, grain size distribution, both free and forced convection and temperature levels play a dominant role in the dissolution process of sand grains during glass melting. Glass tank modelling in combination with glass quality submodelling is still in a stage of development, but these models offer already the possibility to optimize the process conditions in order to obtain a complete melting of the batch, which is one of the major objectives for the glass producer. However, verification of the obtained results and the determination of relevant molten glass properties is essential to make these models more accurate in future and to extend the modelling for the description of homogenization processes, volatilization from the melt, interaction glass melt/refractory and the degassing of the melt [17, 21 and 22].

*

The authors want to thank Dr. J. Peelen and Ir. J. Hermans, Basic Technology Glass of Philips, Eindhoven (The Netherlands), and ir. L. Tromp, PPG Industries Fiber Glass, Hoogezand (The Netherlands), for their support to this work.

## 5. Nomenclature

### 5.1. Symbols

| | |
|---|---|
| $A$ | pre-exponential factor in $s^{-1}$ |
| $B$ | initial temperature of the sand dissolution process in the batch in K |
| $C$ | temperature constant in K |
| $C_1$ | pre-exponential constant in $s^{-1}$ |
| $c_e$ | equilibrium concentration of $SiO_2$ in the melt at the interface of the sand grain in $kg/m^3$ |
| $D_m$ | effective mean diffusivity of $SiO_2$ in the melt in $m^2/s$ |
| $d_p$ | particle diameter in m |
| $Gr$ | Grashof number |
| $g$ | gravity in $m/s^2$ |

$h_d$ mass transfer coefficient controlled by diffusion in m/s
$h_r$ mass transfer coefficient controlled by reaction kinetics in m/s
$h_{rd}$ mass transfer coefficient (without convection) in m/s
$h_{rd1}$ uncorrected mass transfer coefficient in m/s
$R$ radius of sand grain in m
$Re$ Reynolds number
$Sc$ Schmidt number
$Sh$ Sherwood number
$T$ temperature in K
$t$ duration time of the diffusion process in s
$V_s$ specific partial volume of $SiO_2$ in the melt in $m^3/kg$
$v_a$ absolute value of the velocity of a grain relative to the surrounding melt in m/s
$v_s$ ascension by buoyancy in m/s
$v_t$ total velocity of grain relative to local melt velocity in m/s
$v_x$ velocity of melt in $x$ direction in m/s
$v_y$ velocity of melt in $y$ direction in m/s
$v_z$ velocity of melt in $z$ direction in m/s
$w_b$ mass fraction of $SiO_2$ dissolved in the bulk of the melt
$w_e$ mass fraction of dissolved $SiO_2$ in the melt in thermodynamic equilibrium with quartz
$w_{ns}$ mass fraction of $SiO_2$ dissolved in the melt but originating from other constituents than sand
$w_t$ mass fraction of undissolved sand in the glass/sand mixture
$w_0$ mass fraction of undissolved sand in the batch at $t = 0$
$x$ distance in $x$ direction in m
$y$ distance in $y$ direction in m
$z$ distance in $z$ direction in m

$\mu_b$ dynamic viscosity of the bulk of the melt in Pa s
$\varrho_b$ density of the bulk of the melt in $kg/m^3$
$\varrho_e$ density of the melt bounded by the grain surface in $kg/m^3$
$\varrho_s$ density of sand grain in $kg/m^3$

### 5.2. Subscripts

b in the bulk of the melt
d contribution by diffusion
e in the melt at sand grain interface
g free convection
h history term
m average value
mb including moving boundary
ns originating from non-sand materials
ov overall
p particle
r contribution by reaction kinetics
rd including diffusion and reaction kinetics
s in the sand grain
$x$ $x$ direction
$y$ $y$ direction
$z$ $z$ direction

0 at $t = 0$

## 6. References


[1] Benes, J.: The kinetics of silicate glass melting. (Orig. Czech.) Inst. Technology, Prague; thesis 1977.

[2] Hrma, P.; Bartoň, J.; Tolt, T. L.: Interaction between solid, liquid and gas during glass batch melting. J. Non-Cryst. Solids **84** (1986) p. 370–380.

[3] Mühlbauer, M.; Němec, L.: Dissolution of glass sand. Am. Ceram. Soc. Bull. **64** (1985) no. 11, p. 1471–1475.

[4] Beerkens, R.: Kinetik der Quarzsandauflösung in Gemengeteppich und in Glasschmelzen. In: 63. Glastechnische Tagung, Stuttgart 1989. Kurzreferate. Frankfurt/M.: Deutsche Glastech. Ges. 1989. p. 65–70.

[5] Doremus, R. H.: Diffusion of oxygen from contracting bubbles in molten glass. J. Am. Ceram. Soc. **43** (1960) no. 12, p. 655–661.

[6] Weinberg, M. C.; Onorato, P. I. K.; Uhlmann, D. R.: Behavior of bubbles in glassmelts. Pt. 1. Dissolution of a stationary bubble containing a single gas. J. Am. Ceram. Soc. **63** (1980) no. 3–4, p. 175–180.

[7] Readey, D. W.; Cooper, A. R. jr.: Molecular diffusion with a moving boundary and spherical symmetry. Chem. Eng. Sci. **21** (1966) p. 917–922.

[8] Cooper, A. R. jr.; Kingery, W. D.: Dissolution in ceramic systems. Pt. 1. Molecular diffusion, natural convection, and forced convection studies of sapphire dissolution in calcium aluminum silicate. J. Am. Ceram. Soc. **47** (1964) no. 1, p. 37–43.

[9] Choudhary, M. K.: The effect of free convection on the dissolution of a spherical particle in a viscous melt. Glass Technol. **29** (1988) no. 3, p. 100–102.

[10] Choudhary, M. K.: Free convection effects on the dissolution of a spherical particle. In: Advances in the Fusion of Glass. Proc. 1st Int. Conf., Alfred, NY (USA), 1988. p. 11.1–11.23.

[11] Bird, R. B.; Stewart, W. E.; Lightfoot, E. N.: Transport phenomena. New York (et al.): Wiley 1960.

[12] Ungan, A.: Three dimensional numerical simulation of fining process in glass melting furnaces: Mathematical formulation. In: 2nd International Conference on Advances in the Fusion and Processing of Glass, Düsseldorf 1990. Glastech. Ber. **63K** (1990) p. 19–28.

[13] Ungan, A.; Viskanta, R.: Three-dimensional numerical modeling of circulation and heat transfer in a glass melting tank. Pt. 1. Mathematical formulation. Pt. 2. Sample simulation. Glastech. Ber. **60** (1987) no. 3, p. 71–78; no. 4, p. 115–124.

[14] Schill, P.: Calculation of 3-dim. glassmelt flow in large furnaces via twogrid method. In: 2nd International Conference on Advances in the Fusion and Processing of Glass, Düsseldorf 1990. Glastech. Ber. **63K** (1990) p. 39–47.

[15] Waal, H. de: Mathematical modeling of the glass melting process. In: 2nd International Conference on Advances in the Fusion and Processing of Glass, Düsseldorf 1990. Glastech. Ber. **63K** (1990) p. 1–18.

[16] Simonis, F.; Waal, H. de; Beerkens, R. G. C.: Influence of furnace design and operation parameters on the residence time distribution of glass tanks, predicted by 3-D computer simulation. In: XIV International Congress on Glass, New Delhi 1986. Coll. Papers. Vol. 3. p. 118–128.

[17] Beerkens, R. G. C.; Heijden, T. van der; Muijsenberg, E.: Possibilities of glass tank modeling for the prediction of the quality of melting processes. In: 53rd Conference on Glass Problems, Columbus, OH (USA) 1992. Ceram. Eng. Sci. Proc. **14** (1993) no. 3–4, p. 139–160.

[18] Patankar, S. V.: Numerical heat transfer and fluid flow. New York (et al.): McGraw-Hill 1980.

[19] Faber, A. J.; Beerkens, R. G. C.; Waal, H. de: Thermal behaviour of glass batch on batch heating. Glastech. Ber. **65** (1992) no. 7, p. 177–185.

[20] Faber, A. J.; Beerkens, R. G. C.; Waal, H. de: The heating process of glass batch. In: XVI International Congress on Glass, Madrid 1992. Vol. 6. p. 155–160.

[21] Němec, L.: The behaviour of bubbles in glass melts. Pt. 1. Bubble size controlled by diffusion. Pt. 2. Bubble size controlled by diffusion and chemical reaction. Glass Technol. **21** (1980) no. 3, p. 134–138; p. 139–144.

[22] Beerkens, R. G. C.: Chemical equilibrium reactions as driving forces for growth of gas bubbles during refining. In: 2nd International Conference on Advances in the Fusion and Processing of Glass, Düsseldorf 1990. Glastech. Ber. **63K** (1990) p. 222–242.


0794P001